



**HAL**  
open science

## Optical and electrical properties of the transparent conductor SrVO<sub>3</sub> without long-range crystalline order

A. Boileau, A. Cheikh, A. Fouchet, A. David, R. Escobar-Galindo, C. Labbe, P. Marie, F. Gourbilleau, U. Lüders

► **To cite this version:**

A. Boileau, A. Cheikh, A. Fouchet, A. David, R. Escobar-Galindo, et al.. Optical and electrical properties of the transparent conductor SrVO<sub>3</sub> without long-range crystalline order. Applied Physics Letters, 2018, 112 (2), pp.021905. 10.1063/1.5016245 . hal-01693808

**HAL Id: hal-01693808**

**<https://hal.science/hal-01693808>**

Submitted on 26 Jan 2018

**HAL** is a multi-disciplinary open access archive for the deposit and dissemination of scientific research documents, whether they are published or not. The documents may come from teaching and research institutions in France or abroad, or from public or private research centers.

L'archive ouverte pluridisciplinaire **HAL**, est destinée au dépôt et à la diffusion de documents scientifiques de niveau recherche, publiés ou non, émanant des établissements d'enseignement et de recherche français ou étrangers, des laboratoires publics ou privés.

## Optical and electrical properties of the transparent conductor SrVO<sub>3</sub> without long-range crystalline order

A. Boileau,<sup>1</sup> A. Cheikh,<sup>1</sup> A. Fouchet,<sup>1</sup> A. David,<sup>1</sup> R. Escobar-Galindo,<sup>2</sup> C. Labbé,<sup>3</sup> P. Marie,<sup>3</sup> F. Gourbilleau,<sup>3</sup> and U. Lüders<sup>1,a)</sup>

<sup>1</sup>CRISMAT, CNRS UMR6508, ENSICAEN, Normandie Université, 14050 Caen Cedex 4, France

<sup>2</sup>Abengoa Research S. L., Campus Palmas Altas, Calle Energía Solar 1, 41014 Seville, Spain

<sup>3</sup>CIMAP, Normandie Université, ENSICAEN, UNICAEN, CNRS, 14050 Caen Cedex 4, France

(Received 17 November 2017; accepted 26 December 2017; published online 8 January 2018)

It has been shown recently that the perovskite oxide SrVO<sub>3</sub> is a transparent conductor with optical and electrical properties outreaching those of the most used material indium tin oxide (ITO). These properties, observed in the crystalline phase, imply the strong potential of SrVO<sub>3</sub> for use as a lower cost alternative to ITO, but the possible integration of this perovskite oxide material in actual electronic devices is still an open question. One of the possible approaches for the integration of oxide materials is the use of amorphous thin films, allowing low thermal budgets to preserve the performances of the electronic device. Therefore, in this study, the electrical and optical properties of amorphous or poorly crystallized thin SrVO<sub>3</sub> films are investigated. *Published by AIP Publishing.* <https://doi.org/10.1063/1.5016245>

Transparent conducting oxides (TCO) are an important class of materials in a wide range of electronic devices, for example, touch screens, light-emitting diodes, and electrochromic or photovoltaic devices, as they allow for optically transparent electrical contacts.<sup>1–3</sup> The number of known transparent conductors is rather small, as the two main properties, electrical conductivity and optical transparency, are somewhat contradictory. Mobile charge carriers, necessary for the electrical conductivity, absorb light with frequencies below their plasma frequency due to inter- or intraband excitations.<sup>4</sup> Depending strongly on the charge density, the plasma frequency for typical metals is below or above the visible frequencies, while that for some semiconductors such as Sn-doped In<sub>2</sub>O<sub>3</sub> indium tin oxide (ITO),<sup>4</sup> doped ZnO,<sup>5</sup> or a combination thereof<sup>6,7</sup> is below the visible frequencies because of the much lower charge density of around  $1 \times 10^{21} \text{ cm}^{-3}$ .<sup>7</sup> However, the latter feature limits their electrical conduction.

Strongly correlated electronic systems seem to be a way out of this dilemma. With charge densities comparable to those of metals, their plasma frequency is smaller than the visible range because of their enhanced effective electron mass.<sup>8,9</sup> These materials would therefore allow for a high optical transparency and a metallic-like electrical conductivity, as was shown for the two examples SrVO<sub>3</sub> (SVO) and CaVO<sub>3</sub>, at least in the crystalline phase.<sup>8,10</sup> With a carrier concentration in the order of  $2 \times 10^{22} \text{ cm}^{-3}$  and a screened plasma frequency below 1.33 eV, SVO has a remarkable transmission above 60% in the visible window at a thickness of 40 nm and a resistivity close to  $0.5 \times 10^{-4} \Omega \text{ cm}$ .<sup>8</sup> However, the growth conditions used in the cited study are not well adapted to the integration into industrial applications: growth temperatures ranging from 750 °C to 850 °C would be hard to withstand for complex electronic devices. Interdiffusion or decomposition of the device components

may strongly harm the functionalities of the device, at least if the integration of the TCO is needed in the back-end-of-line part of the fabrication.

The aim of this study was therefore to investigate the possibilities of integration of SVO thin films in such devices, with the aim to avoid the constraints of high growth temperature. Crystalline perovskite oxide films are notoriously complicated to be grown on substrates with a different (Si, GaN ...) or without crystal structure (glass, fused silica, polymers, etc.). Therefore, a simple approach lifting the limitations regarding the thermal budget and the mismatch of the crystalline structure is to use the amorphous phase of SVO. This approach is the same as used for ITO, making it a versatile material.<sup>11,12</sup> However, the non-crystalline phase of SVO has not been studied until now, neither in thin films nor in bulk, so that the properties of a disordered SVO are not known.

In this study, SVO thin films were grown on double-side polished (001) oriented (LaAlO<sub>3</sub>)<sub>0.3</sub>(Sr<sub>2</sub>TaAlO<sub>6</sub>)<sub>0.7</sub> (LSAT) substrates, on which high-quality growth was demonstrated before.<sup>8</sup> The growth temperature  $T_G$  has been gradually decreased in order to determine the minimal one for crystalline growth and analyze the resulting properties of the non-crystalline thin films. It has to be noted here that the criterion to distinguish between crystalline and non-crystalline films is the observation of a SVO-related reflection in X-ray Diffraction (XRD). Due to the small volume of the film and the subsequent low intensity of the reflections, small crystalline regions in an amorphous matrix may not lead to visible reflections. Therefore, films not showing SVO-related reflections are called “poorly crystalline” throughout the study, without distinguishing between amorphous, nano-crystalline, and strongly disordered phases. The structural analysis is completed by conductive and optical measurements allowing to judge also on the presence of long-range crystalline order.

SVO thin films have been grown by pulsed laser deposition (PLD) as described in detail elsewhere.<sup>13</sup> The SVO film

<sup>a)</sup>ulrike.luders@ensicaen.fr

thickness was fixed to be around 40 nm for all samples.  $T_G$  has been decreased from 700 °C down to 300 °C. The structural properties and the thickness of the samples were characterized by XRD with a Bruker D8 Advance diffractometer operating with monochromatic Cu  $K_{\alpha 1}$  radiation. Optical properties were measured in the UV-visible-Near Infrared range using a Lambda 1050 Perkin-Elmer spectrophotometer operating in the reflection mode by means of the universal reflectance accessory (URA) and transmission mode. Resistivity and Hall effect were measured with the four-probe method from 5 K to 300 K using the Van der Pauw configuration in a physical properties measurement system (PPMS) by Quantum Design.

Figure 1(a) shows the results of the X-ray diffraction of the SVO thin films for all  $T_G$ . The observation of the SVO (002) peak (marked by vertical arrows) just next to the (002) reflection of the substrate indicates a crystalline state for  $T_G$  from 400 °C on. The sample grown at 300 °C does not show any reflection except the ones from the substrates. If there are crystalline regions in the film, they are too small to be detected with XRD, and no long-range crystalline order is present. Laue fringes are also present in the case of crystalline films. Interestingly, they can be observed already from a growth temperature of 400 °C on, indicating a high crystalline quality in spite of the low growth temperature. Furthermore, long range  $\theta$ - $2\theta$  patterns (not shown here) indicate that the SVO films grown on LSAT are single phased within the limits of detection for the temperature conditions used for the growth.

In the crystalline films, the out-of-plane lattice parameter varies slightly between 3.90 and 3.91 Å, with a roughly monotonous increase with the growth temperature. To get better insight into the structural relation between SVO and LSAT, asymmetrical film reflections were also measured in

skew symmetry. In Fig. 1(b), we present representative reciprocal space maps around (103) Bragg peaks of SVO films grown at 400 °C and 700 °C. The vertical alignment of the reflections indicates a coherently strained state of films with the same in-plane lattice parameter as the one of the LSAT substrate (3.868 Å) within the whole range of deposition temperatures leading to crystallization. Again, we note that the SVO reflection of the sample grown at 400 °C is more intense than the 700 °C one, which confirms the observation of high crystalline quality by the presence of the Laue fringes. The mechanisms behind this unusual dependence of the crystalline quality with  $T_G$  are not entirely understood up to now and will be subject of further studies.

From the literature, the cubic lattice constant of bulk SVO was found to be between 3.82 (Ref. 14) and 3.84 Å.<sup>15–17</sup> In thin films, studies of SVO thin films on the same LSAT substrate have also shown variations between 3.82 Å and 3.84 Å depending on the Sr and V contents.<sup>18</sup> In order to evidence a possible deviation in the cationic contents of SVO films, chemical analyses have been performed by Rutherford backscattering spectrometry with 1.7 MeV He<sup>+</sup> ions (not shown here). The quantification of the Sr/V ratio indicates a maximum variation from the stoichiometric value Sr/V = 1 of 6% between 400 and 700 °C without a clear dependence on the growth temperature, which means an excellent transfer of the cation stoichiometry of the target. However, in the case of our films, the out-of-plane lattice parameter in the same strain state is much larger. This is probably due to the presence of oxygen vacancies in the films, which are generated by the vacuum growth conditions and induced by the tensile strain.<sup>19–21</sup> This is confirmed by the increase in the lattice parameter with the growth temperature [Fig. 1(a)] favoring the apparition of oxygen vacancies. However, as will be discussed later, the influence of these

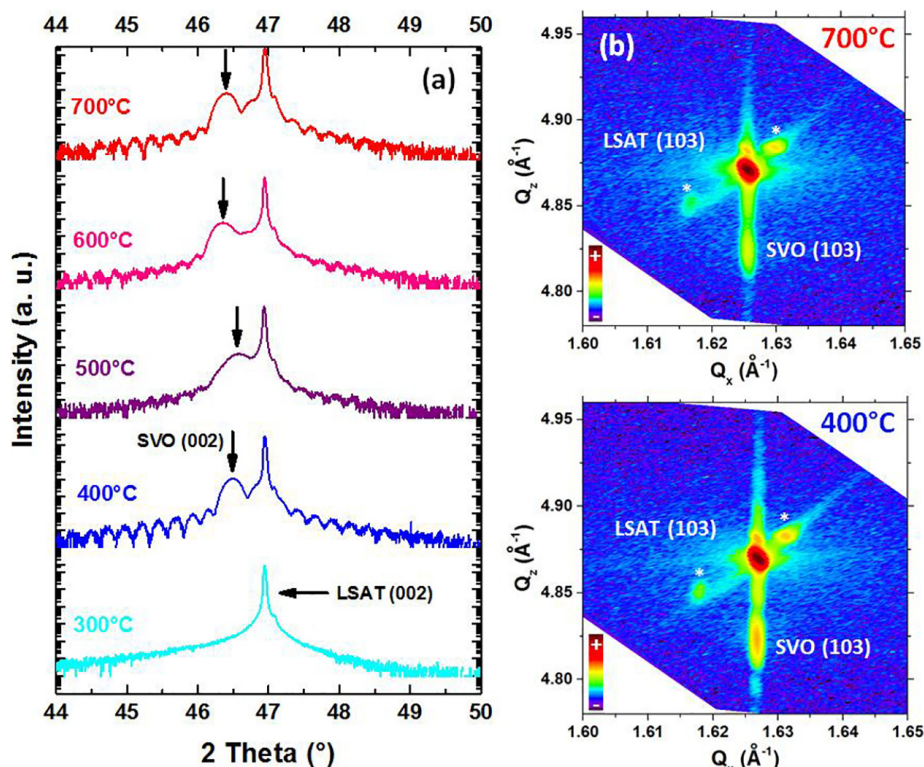


FIG. 1. (a)  $\theta$ - $2\theta$  X-ray diffractograms in the vicinity of the (002) reflection of SrVO<sub>3</sub> thin films grown on LSAT between 300 °C and 700 °C. (b) Reciprocal space maps around the (103) reflection of the films grown at 400 °C and 700 °C. The reflections marked by a star are artefacts due to the diffractometer setup.



oxygen vacancies on the electrical and optical properties remains negligible in contrast to the crystalline order.

The optical transmittance in the visible range is shown in Fig. 2. For all crystalline films, the transmittance has a peak of 80% around 520 nm. At lower wavelength, the transmittance goes down quickly, while at high wavelength, the transmittance remains roughly constant. A slight variation with  $T_G$  can be observed, with a better transmittance for the high  $T_G$  samples. The strong decrease in the transmittance at low wavelength is related to a SVO intraband transition located at around 3.5 eV.<sup>14</sup> This contribution is well confirmed in reflection spectra shown in Fig. 2 by the occurrence of an intense peak located at 400 nm (3.1 eV). The presence of the intraband transition is strongly related to the establishment of extended electronic bands and therefore the periodic structure of the lattice. The absence of this peak in the reflection spectra for the 300 °C sample confirms therefore the absence of a long-range periodic structure, as also observed by XRD. For high wavelengths, absorption is typically due to the mobile charge carriers, especially in the case of strongly correlated systems characterized by a spectral weight transfer of the low lying Drude peak to higher energies.<sup>22</sup> The sample at 300 °C does not show the reduction of transmission, which may be an indication that there are no or only a reduced number of mobile charge carriers in this sample. In the case of crystallized SVO films, a slight depletion of transmission is observed, indicating a stronger contribution of free carriers in SVO grown at or above 400 °C. This point is investigated deeper in the remainder of the study in the light of electrical characterizations.

The resistivity at room temperature for samples grown at different  $T_G$  is shown in Fig. 3. The crystalline films show a resistivity between 1.2 and  $1.9 \times 10^{-4} \Omega \text{ cm}$ , with an increase in the value by lowering  $T_G$ . The temperature dependence of the resistivity of these samples is close to a  $T^2$  behavior as was also observed in the SVO bulk,<sup>23</sup> and the Hall analysis of these samples confirms a charge density ranging from 1.71 (700 °C) to  $2.18 (400 \text{ °C}) \times 10^{22} \text{ cm}^{-3}$  which is very close to the nominal value expected for bulk SVO with one electron per unit cell ( $1.77 \times 10^{22} \text{ cm}^{-3}$ ) and values reported elsewhere in the literature.<sup>8,10,24</sup> Although the charge density increases at low  $T_G$ , the resistivity also increases. By comparing the difference curves in Fig. 3, it is evident that the main difference is an increase in the residual

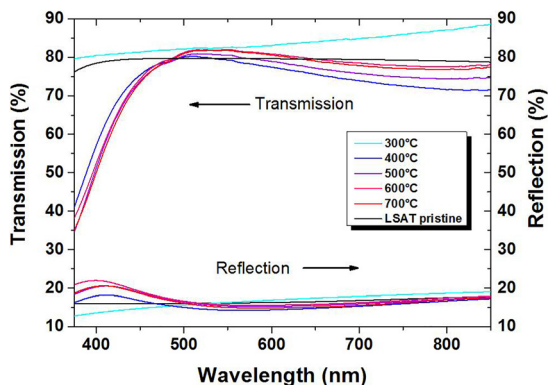


FIG. 2. Transmission and reflection spectra of SrVO<sub>3</sub> thin films grown on LSAT. The pristine substrate is displayed in the figure by the black curve.

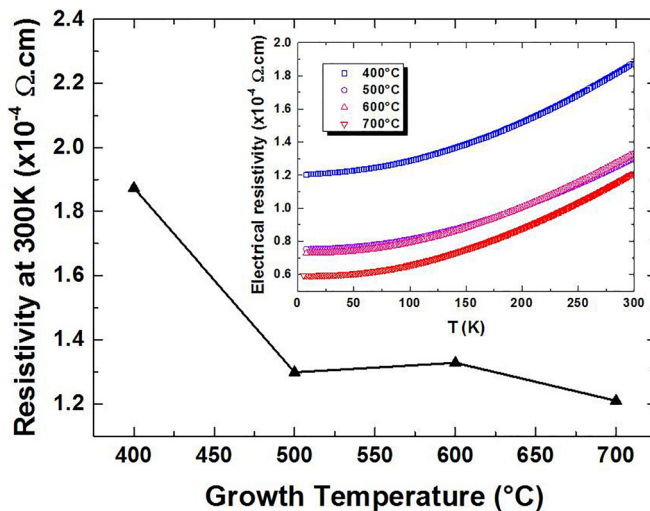


FIG. 3. Evolution of the resistivity of SrVO<sub>3</sub> thin films with the growth temperature measured at room temperature and temperature dependence of the resistivity (inset).

resistivity (i.e., the low-temperature resistivity) at low  $T_G$ , while the temperature-dependent term remains roughly equal. The effect of this enhanced disorder for low  $T_G$  is also visible in the mobility values of the charge carriers, also extracted from the Hall experiments:  $3.05\text{--}1.53 \text{ cm}^2 \text{ V}^{-1} \text{ s}^{-1}$  at high and at low  $T_G$ , respectively. Therefore, the transport in the samples just above the crystallization temperature is governed by strong disorder, leading to enhanced resistivity values.

It was not possible to measure the resistivity of the sample deposited at 300 °C with the experimental setup. However, a lower limit of its resistivity can be estimated to be  $0.1 \Omega \text{ cm}$ , many orders of magnitude higher than the crystalline films. Therefore, the electrical measurements confirm the result of the optical measurements about the absence of mobile charge carriers in the sample grown at 300 °C, i.e., in the poorly crystalline state. This strong discrepancy to the behavior of ITO or semi-conductor based TCOs, being metallic also in the amorphous state,<sup>11,12</sup> is probably due to the orbital character of the involved mobile charge carriers. In SVO, the states at the Fermi energy are of the V  $3d$  type,<sup>25,26</sup> while in the indium-based TCOs, these bands have a  $5s$  character.<sup>4</sup> The  $s$  orbitals are much less anisotropic in space than the  $3d$  orbitals, so that some overlap is still possible in the amorphous  $5s$  system. In the case of strongly disordered  $3d$  systems, the absence of the overlap of the vanadium and oxygen orbitals inhibits long-range electrical conduction. Several studies deal with transition metal  $3d$  type vanadates exhibiting a semi-conducting behavior with clear localization of carriers. For example, it is well-known that the conduction in the V<sub>2</sub>O<sub>5</sub> amorphous phase is ensured by a hopping process.<sup>27,28</sup> However, in our case, SrVO<sub>3</sub> is a vanadate showing metallic conduction, i.e., delocalized charges. The delocalization of the charges may reduce their orbital character and render the electrical transport less sensitive to its crystalline state. Another strongly correlated  $4f$  system, SrRuO<sub>3</sub>, shows a metallic to insulating transition with the leaking of the crystalline phase around 300–400 °C.<sup>29</sup> The authors suggest a hopping mechanism to explain the  $T^{1/4}$

dependence of the resistivity in amorphous films. For this reason, with the non-accessible resistivity curve for SVO deposited at 300 °C, a hopping process cannot be totally excluded and further investigations are needed to point out the transport in amorphous SVO.

In conclusion, the study of the properties of SVO thin films grown at temperatures between 300 °C and 700 °C has shown that SVO thin films lacking long-range structural order are insulating. However, the system crystallizes at a remarkably low temperature of 400 °C on an adapted substrate, showing electrical and optical properties being comparable to those of other TCOs. Therefore, SVO will not be easy to integrate into complex electronic devices at least not in the back-end-of-line, but the low crystallization temperature of SVO and the comparable performances with state-of-the-art TCOs would allow for a low cost and efficient front-end-of-line integration.

The sample grown at 400 °C, just above the crystallization threshold, will be investigated further. Showing in the XRD measurements a crystalline quality comparable to the sample grown at 700 °C, the resistance measurements however indicate a higher density of scattering centers for the mobile charge carriers. As these scattering centers are usually related to some kind of disorder and especially disorder of the crystalline structure, these two observations seem to be contradictory. More studies are needed in order to determine the exact nature of the scattering centers, which may also help to eliminate a part of them enhancing the conductivity of the low  $T_G$  samples.

The authors thank the Labex EMC3 (Energy Materials and Clean Combustion Center) for its financial support in the framework of the COTRA Project and express their gratitude to Daniel Janke from the Ion Beam Center, Helmholtz Zentrum Dresden Rossendorf for his participation to Rutherford backscattering spectrometry measurements. The authors thank also M. Boisserie and C. Frilay for important technical help on the electrical and optical measurements, respectively.

<sup>1</sup>C. G. Granqvist, *Sol. Energy Mater. Sol. Cells* **91**, 1529 (2007).

<sup>2</sup>E. Fortunato, D. Ginley, H. Hosono, and D. C. Paine, *MRS Bull.* **32**, 242 (2007).

- <sup>3</sup>S. C. Dixon, D. O. Scanlon, C. J. Carmalt, and I. P. Parkin, *J. Mater. Chem. C* **4**, 6946 (2016).
- <sup>4</sup>O. Mryasov and A. Freeman, *Phys. Rev. B* **64**, 233111 (2001).
- <sup>5</sup>K. Ellmer, *J. Phys. Appl. Phys.* **33**, R17 (2000).
- <sup>6</sup>A. J. Freeman, K. R. Poeppelmeier, T. O. Mason, R. P. H. Chang, and T. J. Marks, *MRS Bull.* **25**, 45 (2000).
- <sup>7</sup>T. Minami, *Semicond. Sci. Technol.* **20**, S35 (2005).
- <sup>8</sup>L. Zhang, Y. Zhou, L. Guo, W. Zhao, A. Barnes, H.-T. Zhang, C. Eaton, Y. Zheng, M. Brahlek, H. F. Haneef *et al.*, *Nat. Mater.* **15**, 204 (2015).
- <sup>9</sup>K. R. Poeppelmeier and J. M. Rondinelli, *Nat. Mater.* **15**, 132 (2016).
- <sup>10</sup>M. Gu, S. A. Wolf, and J. Lu, *Appl. Phys. Lett.* **103**, 223110 (2013).
- <sup>11</sup>H. Morikawa and M. Fujita, *Thin Solid Films* **359**, 61 (2000).
- <sup>12</sup>F. Kurdesau, G. Khripunov, A. F. da Cunha, M. Kaelin, and A. N. Tiwari, *J. Non-Cryst. Solids* **352**, 1466 (2006).
- <sup>13</sup>Q.-R. Li, M. Major, M. B. Yazdi, W. Donner, V. H. Dao, B. Mercey, and U. Lüders, *Phys. Rev. B* **91**, 035420 (2015).
- <sup>14</sup>H. Makino, I. H. Inoue, M. J. Rozenberg, I. Hase, Y. Aiura, and S. Onari, *Phys. Rev. B* **58**, 4384 (1998).
- <sup>15</sup>M. J. Rey, P. Dehault, J. C. Joubert, B. Lambert-Andron, M. Cyrot, and F. Cyrot-Lackmann, *J. Solid State Chem.* **86**, 101 (1990).
- <sup>16</sup>T. Maekawa, K. Kurosaki, and S. Yamanaka, *J. Alloys Compd.* **426**, 46 (2006).
- <sup>17</sup>K.-J. Range, F. Rau, and U. Klement, *Z. Naturforsch. B* **46**, 1315 (1991).
- <sup>18</sup>J. A. Moyer, C. Eaton, and R. Engel-Herbert, *Adv. Mater.* **25**, 3578 (2013).
- <sup>19</sup>G. Herranz, M. Basletić, O. Copie, M. Bibes, A. N. Khodan, C. Carrétéro, E. Tafrá, E. Jacquet, K. Bouzouhane, A. Hamzić *et al.*, *Appl. Phys. Lett.* **94**, 012113 (2009).
- <sup>20</sup>O. Copie, H. Rotella, P. Boullay, M. Morales, A. Pautrat, P.-E. Janolin, I. C. Infante, D. Pravathana, U. Lüders, and W. Prellier, *J. Phys. Condens. Matter* **25**, 492201 (2013).
- <sup>21</sup>J. R. Petrie, C. Mitra, H. Jeon, W. S. Choi, T. L. Meyer, F. A. Reboredo, J. W. Freeland, G. Eres, and H. N. Lee, *Adv. Funct. Mater.* **26**, 1564 (2016).
- <sup>22</sup>D. N. Basov, R. D. Averitt, D. van der Marel, M. Dressel, and K. Haule, *Rev. Mod. Phys.* **83**, 471 (2011).
- <sup>23</sup>M. Onoda, H. Ohta, and H. Nagasawa, *Solid State Commun.* **79**, 281 (1991).
- <sup>24</sup>A. Fouchet, M. Allain, B. Bérini, E. Popova, P.-E. Janolin, N. Guiblin, E. Chikoidze, J. Scola, D. Hrabovsky, Y. Dumont *et al.*, *Mater. Sci. Eng. B* **212**, 7 (2016).
- <sup>25</sup>Y. Aiura, F. Iga, Y. Nishihara, H. Ohnuki, and H. Kato, *Phys. Rev. B* **47**, 6732 (1993).
- <sup>26</sup>I. A. Nekrasov, G. Keller, D. E. Kondakov, A. V. Kozhevnikov, T. Pruschke, K. Held, D. Vollhardt, and V. I. Anisimov, *Phys. Rev. B* **72**, 155106 (2005).
- <sup>27</sup>M. Henri, C. Sanchez, C. R. Kha, and J. Livage, *J. Phys. C: Solid State Phys.* **14**, 829 (1981).
- <sup>28</sup>C. Sanchez, R. Morineau, and J. Livage, *Phys. Status Solidi* **76**, 661 (1983).
- <sup>29</sup>J. Y. Son, B. G. Kim, and J. H. Cho, *Thin Solid Films* **515**, 7086 (2007).